doi:10.1017/S1431927615003529 Paper No. 0273 Microsc. Microanal. 21 (Suppl 3), 2015

Exploiting the Susceptibility of HIV-1 Nucleocapsid Protein to Radiation Damage in Tomo-Bubblegram Imaging.

Juan Fontana[1], Kellie A. Jurado[2], Naiqian Cheng[1], Alan Engelman[2], and Alasdair C. Steven[1].

[1] Laboratory of Structural Biology Research, National Institute of Arthritis, Musculoskeletal and Skin Diseases, National Institutes of Health, Bethesda, MD 20892, USA
[2] Department of Cancer Immunology and AIDS, Dana-Farber Cancer Institute, Boston, MA 02215, USA

During HIV-1 maturation, a process required for viral infectivity, the capsid protein CA assembles into a conical shell that is thought to contain the viral ribonucleoprotein (vRNP) complex comprised of the viral RNA (vRNA) and nucleocapsid protein NC. Maturation is inhibited by different classes of antiHIV drugs, including allosteric integrase inhibitors (ALLINIs) [1]. To further understand the maturation process and the mode of action of these drugs, we imaged HIV-1 virions produced in the presence of ALLINIs by cryo-electron tomography (cryo-ET) and "tomo-bubblegram" imaging. The latter is a novel labeling technique that extends "bubblegram imaging" [2, 3] into three dimensions. In the HIV-1 system, we found that it exploits the exceptional susceptibility of NC to radiation damage.

Bubblegram imaging takes advantage of the fact that vitrified protein specimens subjected to relatively high levels of electron irradiation generate bubbles of hydrogen gas that are readily visible. Moreover, proteins in complex with DNA bubble relatively early because the DNA impedes the diffusion of radiation products, accelerating the formation of bubbles. Hypothesizing that some component(s) of HIV may have distinctive bubbling behavior, we visualized HIV-1 virions in this way, and found that bubbles started to appear after a cumulative dose of ~160-200 $e^-/Å^2$. We then extended the approach to tomo-bubblegrams. First, a regular tilt-series was collected and a tomogram was calculated (total dose of ~75 $e^-/Å^2$). Second, an untilted dose-series was performed, stopping after the first bubbles began to develop (another ~70 $e^-/Å^2$). Third, after waiting ~2 h to allow radiation products to dissipate, a second tilt series was recorded (~70 $e^-/Å^2$), allowing the visualization of the bubbles in the "tomo-bubblegram".

Imaged by cryo-ET (Figure 1), most wild-type virions have conical cores with internal density that is thought to be the vRNP. In contrast, ALLINI-treated virions have few such cores and instead contain "eccentric condensates", spheroidal aggregates that are located outside of the capsid and close to the viral envelope [1]. When an ALLINI-treated virion contains both an eccentric condensate and a conical core, the core is relatively empty (cf. Figures 1A & B). In virions visualized by bubblegram imaging, the bubbles co-project with core interiors and eccentric condensates, and the two structures have the same bubbling threshold (Figure 2). Tomo-bubblegram imaging confirms that the bubbles specifically label the contents of filled cores and the eccentric condensates (Figures 3A & B). To further clarify which virion component is bubbling, we examined immature virions, which have a thick-walled shell in which the domains of the polyproteins Gag and Gag-Pol are radially ordered. Here, the bubbles appear in the inner part of that shell (Figure 3C). The interpretation of NC as the bubbling component was further supported by analyses of Gag/ψ-minus particles, which do not incorporate vRNA, (Figure 3D); of Gag-LeuZip particles, in which the NC domain is replaced by a leucine zipper (Figure 3E); and of purified recombinant NC protein (not shown). Taken together, these observations provide strong evidence that ALLINIs act by sabotaging capsid assembly and vRNP encapsidation. They also show that proteins differ in their bubbling thresholds and that nucleic acid is not needed to induce bubbling.

References:

[1] KA Jurado et al., Proc Natl Acad Sci U S A **110** (2013), 8690-5.
[2] W Wu et al., Science **335** (2012), 182.
[3] N Cheng et al., J Struct Biol **185** (2014), 250-6.
[4] This work was funded in part by the Intramural Research Program of NIAMS (A.C.S.), the Intramural AIDS Targeted Antiviral Program (A.C.S), and National Institutes of Health grants AI070042 and GM103368 (A.E.).

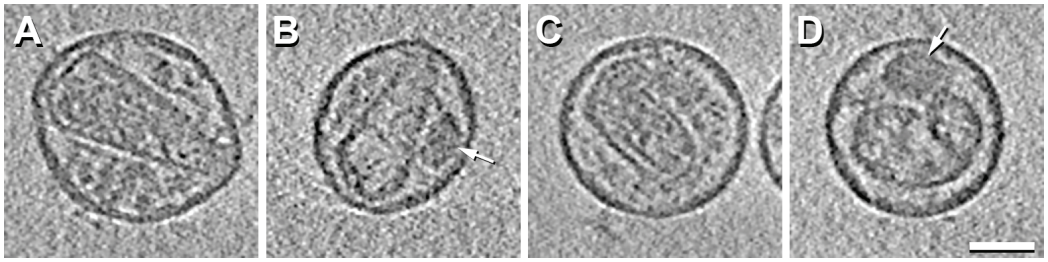

Figure 1. Tomographic central slices of HIV-1 virions classified according to core morphology (conical or non-conical) and the presence (white arrows) or absence of an eccentric condensate. Bar, 50 nm.

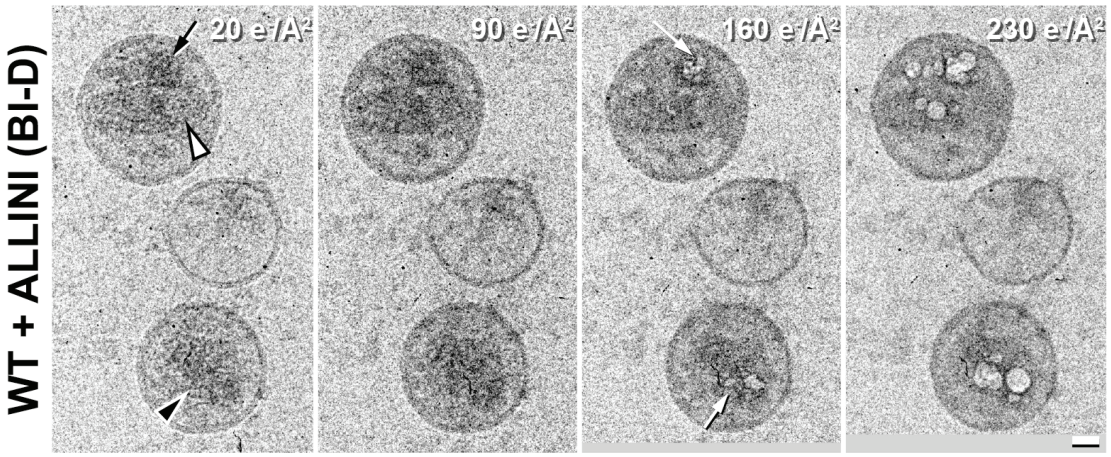

Figure 2. Bubblegram imaging. Black arrowhead, filled core; white arrowhead, core with less content; black arrow, eccentric aggregate; white arrows, first bubbles. Bar, 50 nm.

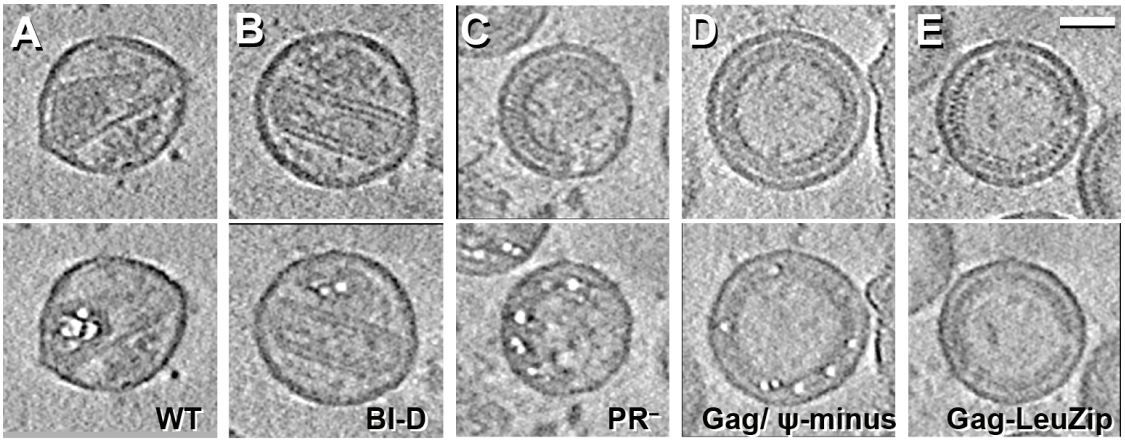

Figure 3. Tomo-bubblegrams. Each pair of panels shows a central section from the initial tomogram (top) and the corresponding section from the tomo-bubblegram (bottom). Bar, 50 nm.

https://doi.org/10.1017/S1431927615003529 Published online by Cambridge University Press